APPLIED AND ENVIRONMENTAL MICROBIOLOGY, July 1996, p. 2577–2585 Vol. 62, No. 7
0099-2240/96/$04.00+0

Citrate and Sugar Cofermentation in *Leuconostoc oenos*, a ^{13}C Nuclear Magnetic Resonance Study

ANA RAMOS[1] AND HELENA SANTOS[1,2]*

Instituto de Tecnologia Química e Biológica/Universidade Nova de Lisboa, 2780 Oeiras,[1] and Departamento de Química, Faculdade de Ciências e Tecnologia U.N.L., Universidade Nova de Lisboa, 2825 Monte de Caparica,[2] Portugal

Received 15 December 1995/Accepted 13 April 1996

^{13}C nuclear magnetic resonance spectroscopy was used to investigate citrate-glucose cometabolism in nongrowing cell suspensions of the wine lactic acid bacterium *Leuconostoc oenos*. The use of isotopically enriched substrates allowed us to identify and quantify in the end products the carbon atoms derived from each of the substrates supplied; furthermore, it was possible to differentiate between products derived from the metabolism of endogenous carbon reserves and those derived from external substrates. Citrate-sugar cometabolism was also monitored in dilute cell suspensions for comparison with the nuclear magnetic resonance results. A clear metabolic shift of the end products from glucose metabolism was observed when citrate was provided along with glucose: ethanol was replaced by acetate, and 2,3-butanediol was produced. Reciprocally, the production of lactate and 2,3-butanediol from citrate was increased in the presence of glucose. When citrate was cometabolized with glucose, a 10-fold reduction in the intracellular concentration of glucose-6-phosphate was observed, a result in line with the observed citrate-induced stimulation of glucose consumption. The presence of citrate provided additional pathways for $NADP^+$ regeneration and allowed the diversion of sugar carbon to reactions in which ATP was synthesized. The increased growth rates and maximal biomass yields of *L. oenos* growing on citrate-glucose mixtures resulted from increased ATP synthesis both by substrate-level phosphorylation and by a chemiosmotic mechanism.

Reports on the alteration of the pattern of fermentation products in lactic acid bacteria as a result of mixotrophic conditions are common in the literature (2, 10, 13, 25). Because of the complexity of the media in which natural fermentations occur (e.g., milk, wine, and meat), strong metabolic interactions between the multiple substrates are expected. Citrate and sugar metabolism, as well as the effects derived from the presence of mixed substrates, has been widely studied in strains of both homofermentative and heterofermentative lactic acid bacteria relevant to the dairy industry, such as *Lactococcus lactis*, *Leuconostoc mesenteroides*, and *Leuconostoc lactis*, mainly because of the importance of diacetyl as a flavor compound in dairy products (2, 3, 15, 21–23). These studies have reported on growth stimulation, alterations in the substrate uptake rates, and molar ratios of the end products caused by the additional presence of citrate. However, much less attention has been devoted to sugar-citrate cometabolism in nondairy lactic acid bacteria involved in wine production.

To improve the properties of wine, it is important to characterize the metabolism of the organisms involved in the production process. *Leuconostoc oenos* is the major species performing malolactic fermentation at the low pH values found in wine. During fermentation, residual carbohydrates (mainly glucose, fructose, and arabinose at concentrations up to 10 mM after alcoholic fermentation) and citrate (1 to 5 mM) are metabolized (18), leading to the production of compounds, such as diacetyl, that add to the organoleptic properties of wine (4, 6, 27). In the studies of sugar-citrate cometabolism by *L. oenos* (11, 12, 20), interpretation of the results is often difficult since the two substrates have a common intermediate metabolite, pyruvate, and therefore the origin of the end products cannot be determined with precision. Furthermore, in many studies, not all the end products were determined, and often the redox balance was not useful, most probably because of leakage of electrons to oxygen via the NAD(P)H oxidases. Therefore, the information supplied by the majority of the analytical methods available is insufficient to fully describe cometabolic processes. Nuclear magnetic resonance spectroscopy (NMR) is an attractive technique for these studies, since the fate of ^{13}C-enriched substrates can be monitored noninvasively throughout the metabolic pathways. Furthermore, the origin of the carbon atoms in the end products formed under mixotrophic conditions can be determined by analysis of their labeling patterns (15, 24).

In the present study, we report on the relationships between sugar and citrate metabolism in *L. oenos*. Both NMR and other analytical techniques were used to quantify end products and to determine carbon fluxes. The accumulation of phosphorylated metabolites under different metabolic conditions was evaluated by ^{31}P-NMR. The effect of citrate on energy conservation was evaluated in both nongrowing and growing cells.

MATERIALS AND METHODS

Organism and growth conditions. *L. oenos* GM (Microlife Techniques, Sarasota, Fla.) was grown in FT80 medium, containing (per liter) 5 g of Casamino Acids, 4 g of yeast extract, 0.6 g of KH_2PO_4, 0.5 g of KCl, 0.1 g of $CaCl_2$, 0.1 g of $MgSO_4 \cdot 7H_2O$, 3 mg of $MnSO_4 \cdot H_2O$, 8 g of glucose, and 2.5 g of citrate, as described previously (16). Manganese was omitted from the culture medium when the cells were grown for perchloric acid extraction. For the evaluation of growth of *L. oenos* on citrate alone, FT80 medium without added glucose or a defined medium was used (19).

Growth measurements and quantification of cell dry mass. Growth was determined by measuring the optical density of the culture at 600 nm (OD_{600}). Samples were diluted when necessary to allow the absorbance reading to fall between 0.05 and 0.7. In this range, the absorbance was directly proportional to the biomass concentration. The dry cell mass concentration (DM) was determined from the OD reading by using the equation $DM = 0.46\ OD_{600}$. The constant 0.46 is the slope of a standard curve of dry cell mass (in milligrams per milliliters) versus OD_{600}.

Sample preparation for NMR experiments. Cells were harvested by centrifu-

* Corresponding author. Mailing address: Instituto de Tecnologia Química e Biológica/Universidade Nova de Lisboa, Rua da Quinta Grande, 6, Apt. 127, 2780 Oeiras, Portugal. Phone: 351-1-4426171 Fax: 351-1-4428766. Electronic mail address: santos@itqb.unl.pt.

gation (2,000 × *g* for 10 min at 4°C), washed twice with 50 mM potassium phosphate (pH 4.0), and resuspended in the same solution to approximately 15 mg (dry mass) of cells · ml^{-1}. The cell suspension (3.5 ml) was immediately transferred to a 10-mm NMR tube; ^2H_2O (5%, vol/vol) was added to provide a lock signal, and the ^{13}C-labeled substrates were added. The time course for substrate consumption and product formation was monitored in vivo by ^{13}C-NMR. All experiments were run at a probe head temperature of 30°C. Once the citrate had been exhausted, the acquisition was stopped, the cells were centrifuged (30,000 × *g* for 30 min at 4°C), and the supernatant solution was saved; the cell pellet was washed once with buffer and centrifuged again, and the two fractions were pooled. Supernatant solutions were kept at −20°C until analyzed by ^{13}C- and ^1H-NMR.

Sample preparation for experiments with dilute cell suspensions. Cells were harvested and resuspended in 50 mM potassium phosphate to a final pH of 4.0 and to approximately 3 mg (dry mass) of cells · ml^{-1}. The cell suspension (30 ml) was incubated in a water bath at 30°C and stirred gently under a continuous flow of nitrogen. The substrates were added, and samples were taken at time intervals following the addition and immediately centrifuged (2,000 × *g* for 10 min at 4°C). The supernatant solutions were kept at −20°C until further analysis.

NMR spectroscopy. ^{13}C- and ^1H-NMR spectra were recorded as previously described (16). ^{31}P spectra were acquired at 202.45 MHz with the following acquisition parameters: spectral width, 20 kHz; pulse width, 10 μs (corresponding to a 45° flip angle); data size, 32K; repetition delay, 20 s; number of scans, 3,000.

Quantification of products in the supernatant solutions. Glucose and fructose were measured by using the appropriate test combination kits supplied by Boehringer Mannheim, Inc. Arabinose was determined by high-performance liquid chromatography as described previously (23). Citrate, acetate, lactate, acetoin, and 2,3-butanediol were quantified by proton NMR, as previously described (16). In the experiments involving labeled substrates, the isotopic enrichment in the methyl groups was evaluated directly from ^1H-NMR spectra; enrichment in the other carbon atoms of acetate, lactate, and 2,3-butanediol was determined from fully relaxed ^{13}C-NMR spectra of the supernatant solutions. The kinetic data shown in Fig. 4 were extracted from the in vivo ^{13}C spectra obtained during the consumption of [2-^{13}C]glucose in the following way: the absolute concentrations of [^{13}C]acetate and [^{13}C]ethanol were determined from proton NMR analysis of the liquid supernatant obtained at the end of the experiment, and in the calculations it was assumed that the products present at the end of the NMR experiments were fully recovered in the supernatants by the procedure described above.

Preparation of perchloric acid extracts and quantification of phosphorylated metabolites. Cells were grown and harvested by centrifugation, washed twice with 50 mM potassium phosphate (pH 4.0) and resuspended to a final volume of 10 ml in 50 mM glycine buffer (pH 3.5). Cell suspensions were transferred to a test tube and placed in a water bath at 30°C, and the substrates were added. After 10 min, the cells were quickly frozen in liquid nitrogen by dispersion with a syringe to minimize changes in intracellular metabolites. The frozen cell aggregates were collected and used for perchloric acid extraction, as previously described (9). For each extract, approximately 1 g (dry mass) of cells was used. The pH of the extracts was adjusted to 8.0 by addition of NaOH, and 4 mM (final concentration) EDTA was added before the analysis by ^{31}P-NMR. Spectra were run with the acquisition parameters described above, and the resonances of phosphorylated metabolites were assigned by addition of the pure compounds. The quantification was made with methylphosphophonic acid as the internal standard, added to the extracts to a final concentration of 0.5 mM.

ATP determination. Cells were harvested as described above and resuspended in 50 mM potassium phosphate (pH 4.0) to approximately 1 mg (dry mass) of cells · ml^{-1}. The cell suspensions were incubated at 30°C, the substrates were added, and samples were taken at time intervals following the addition. After extraction with perchloric acid and neutralization, the ATP concentration in the samples was measured by the luciferin-luciferase assay described previously (14).

Chemicals. [2,4-^{13}C]citrate (100% enriched) was supplied by Advanced Research on Chemistry, Amsterdam, The Netherlands. [2-^{13}C]glucose (99%) and [5-^{13}C]glucose (99%) were supplied by Omicron Biochemicals Inc., South Bend, Ind. Formic acid was purchased from Merck, and methylphosphonic acid was supplied by Sigma Chemical Co., Ltd. All other chemicals were of reagent grade.

RESULTS

Effect of citrate on growth of *L. oenos*. The influence of citrate on the growth rate of and the maximal biomass concentration reached by *L. oenos* was investigated. Citrate in the concentration range of 0 to 50 mM was added to the growth medium (pH 4.8) containing 8 g of glucose · $liter^{-1}$ (45 mM). Citrate had a drastic effect on the specific growth rate, as well as on the maximal biomass concentration reached (Fig. 1). The specific growth rate increased from 0.003 h^{-1} in the absence of citrate to 0.04 or 0.05 h^{-1} when 10 or 20 mM citrate was added to the growth medium, respectively. The maximal biomass concentration increased from 0.03 to 0.5 mg of dry cell mass · ml^{-1} when the citrate concentration was increased from 0 to 20 mM. Growth was also monitored on FT80 medium without an added carbon source or with citrate (10 mM), and significantly higher turbidity was observed in citrate-containing medium (data not shown). However, attempts to grow *L. oenos* on defined medium with citrate as the sole carbon source have been unsuccessful so far.

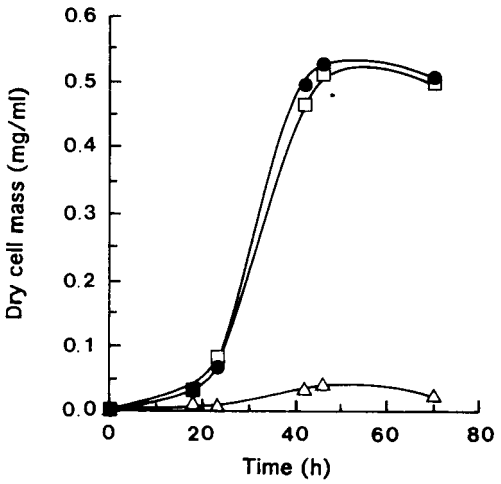

FIG. 1. Effect of citrate on the growth of *L. oenos*. Growth was measured in medium containing glucose (45 mM) at 30°C and pH 4.8. Symbols: □, 10 mM citrate; ●, 20 mM citrate; △, no citrate added.

Citrate-sugar cometabolism monitored in dilute cell suspensions. Citrate-glucose, citrate-fructose, or citrate-arabinose cometabolism was monitored in dilute cell suspensions at pH 4.0, and the kinetics of substrate utilization and product formation are shown in Fig. 2. Product formation from citrate as the sole carbon source (5 mM) under the same experimental conditions is also shown for comparative purposes. The rate of citrate consumption in dilute cell suspensions, 150 μmol · min^{-1} · g (dry mass) of $cells^{-1}$, was not affected by the presence of a cosubstrate. Glucose and fructose were consumed at 120 and 35 μmol · min^{-1} · g (dry mass) of $cells^{-1}$, respectively, provided that citrate was present. After citrate exhaustion, the rate of glucose utilization decreased to 35 μmol · min^{-1} · g (dry mass) of $cells^{-1}$ whereas the rate of fructose consumption remained constant. The end products with citrate as the sole carbon source were acetate, lactate, and acetoin; only trace amounts of 2,3-butanediol were produced. However, when glucose or fructose was supplied in addition to citrate, the pattern of product formation was changed, with the end products being acetate, lactate, and 2,3-butanediol. During citrate-fructose cometabolism, acetoin was transiently detected and further metabolized to 2,3-butanediol. The pattern of product formation from citrate plus arabinose, consumed at a rate of 20 μmol · min^{-1} · g (dry mass) of $cells^{-1}$, was significantly different from that from citrate-hexose cometabolism; acetoin was found as an end product in addition to acetate and lactate, and only trace amounts of 2,3-butanediol were produced. Carbon recoveries in these experiments varied between 85 and 115%. Values above 100% occur because significant amounts of acetate and lactate produced were derived from endogenous reserve compounds, as previously shown (16).

Effect of citrate on glucose metabolism. According to the metabolic pathways shown in Fig. 3, the ^{13}C-labeled products expected from the metabolism of [2-^{13}C]glucose are [2-^{13}C]ac-

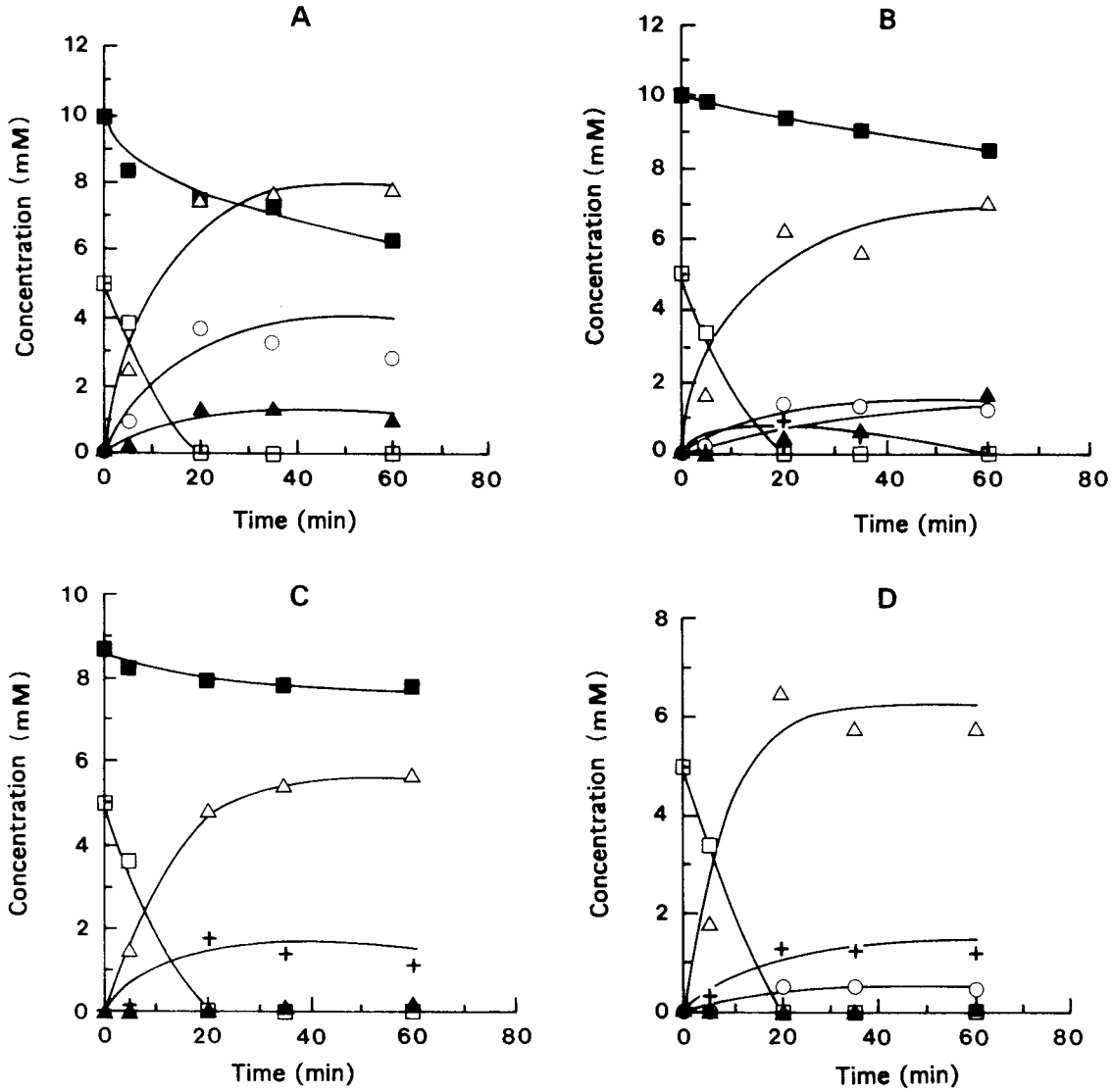

FIG. 2. Kinetics of substrate consumption and product formation in dilute cell suspensions at pH 4.0 from citrate-glucose (A), citrate-fructose (B), citrate-arabinose (C), and citrate alone (D). Symbols: □, citrate; ■, glucose, fructose, or arabinose; △, acetate; ○, lactate; +, acetoin; ▲, 2,3-butanediol.

etate and [2-^{13}C]ethanol. The metabolism of glucose labeled at the C-2 position (12 mM) by a cell suspension of *L. oenos* was monitored by ^{13}C-NMR, and the results are shown in Fig. 4. The initial glucose consumption rate was 30 μmol · min^{-1} · g (dry mass) of cells^{-1}, and the end products were acetate and ethanol (1:1 molar ratio) isotopically enriched in the respective methyl groups. At the time indicated (arrow), unlabeled citrate (5 mM) was added and a new set of spectra were acquired. The addition of citrate caused a twofold stimulation of the rate of glucose metabolism and a clear metabolic shift toward the production of acetate; in fact, ethanol formation ceased, and acetate was the only labeled metabolite formed from glucose. Proton NMR was used to quantify and evaluate the isotopic enrichment on the end products present in the supernatant solutions obtained from these experiments (results not shown), as described previously (15). In addition to the labeled acetate and ethanol, unlabeled lactate, acetate, and 2,3-butanediol were detected. No acetoin was detected, a result which is consistent with the pattern of product formation from citrate in the presence of glucose or fructose found in dilute cell suspensions. This experiment is a clear illustration of the citrate-induced shift in the end products of glucose catabolism, but it did not allow us to distinguish the products derived from each substrate, since unlabeled compounds were produced from both the unlabeled citrate and the nonlabeled moiety of glucose. Furthermore, the contribution of metabolites produced from the mobilization of endogenous reserve compounds could not be assessed.

Cometabolism of isotopically labeled citrate and glucose monitored by ^{13}C-NMR. To distinguish the end products derived from the metabolism of citrate from those produced from glucose and also from the metabolites derived from reserve compounds, it was necessary to use both selectively ^{13}C-labeled citrate and glucose. The cometabolism of equimolar amounts of [2-^{13}C]glucose–[5-^{13}C]glucose (15 μmol each) and [2,4-^{13}C]citrate (15.9 μmol) at pH 4.0 was probed in vivo by ^{13}C-NMR (data not shown). Citrate and glucose were consumed at 67 and 26 μmol · min^{-1} · g (dry mass) of cells^{-1}, respectively.

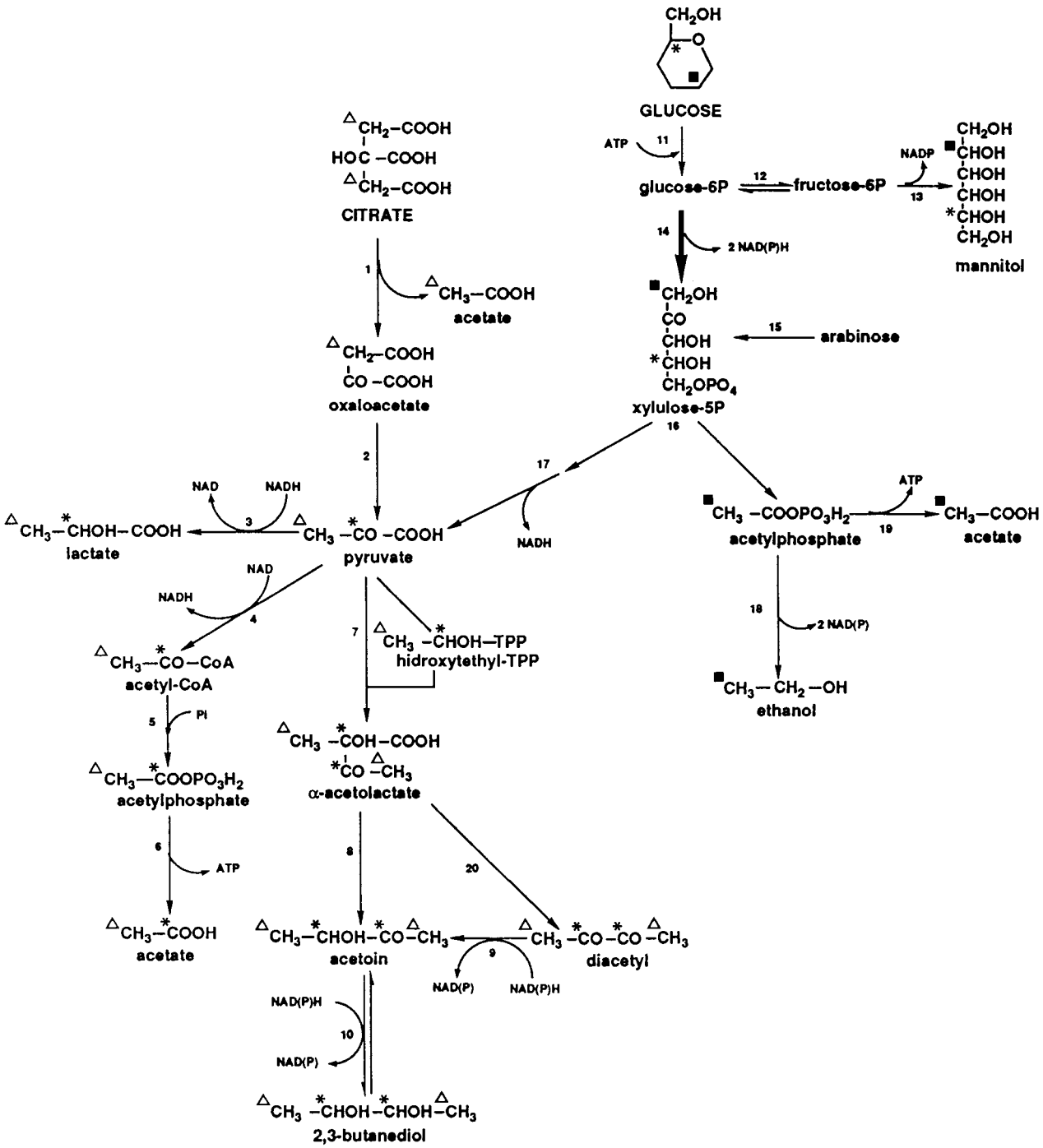

FIG. 3. Metabolic pathways of citrate and glucose breakdown by *L. oenos*. 1, citrate lyase; 2, oxaloacetate decarboxylase; 3, lactate dehydrogenase; 4, pyruvate dehydrogenase complex; 5, phosphotransacetylase; 6, acetate kinase; 7, α-acetolactate synthase; 8, α-acetolactate decarboxylase; 9, diacetyl reductase; 10, acetoin reductase; 11, hexokinase; 12, glucose-6-phosphate isomerase; 13, mannitol dehydrogenase; 14, glucose-6-phosphate dehydrogenase, 6-phosphogluconate dehydrogenase, and ribulose-5-phosphate epimerase; 15, arabinose ketol-isomerase, ATP:ribulose 5-phosphotransferase, and ribulose 5-phosphate 4-epimerase; 16, phosphoketolase; 17, enzymes as in the Embden-Meyerhof-Parnas pathway; 18, phosphotransacetylase, acetaldehyde dehydrogenase, and alcohol dehydrogenase; 19, acetate kinase; 20, nonenzymatic decarboxylative oxidation of α-acetolactate. TPP, thiamine pp_i. The labeling patterns on the intermediates and end products derived from the metabolism of [2,4-^{13}C]citrate (△), [2-^{13}C]glucose (■), and [5-^{13}C]glucose (*) are shown.

Once citrate was completely metabolized, the liquid supernatants were obtained and analyzed by ^{13}C- and ^{1}H-NMR (Fig. 5); enzymatic determinations of glucose concentration showed that only 10.2 μmol was used. Acetoin and ethanol were not detected in the carbon spectra acquired in vivo or in the carbon or proton spectra of the supernatant solutions. In the proton spectra (Fig. 5) of supernatant solutions containing the end products of citrate-glucose cometabolism, the resonance patterns due to the methyl groups of acetate, lactate, and 2,3-butanediol were assigned. With the resonance pattern of ace-

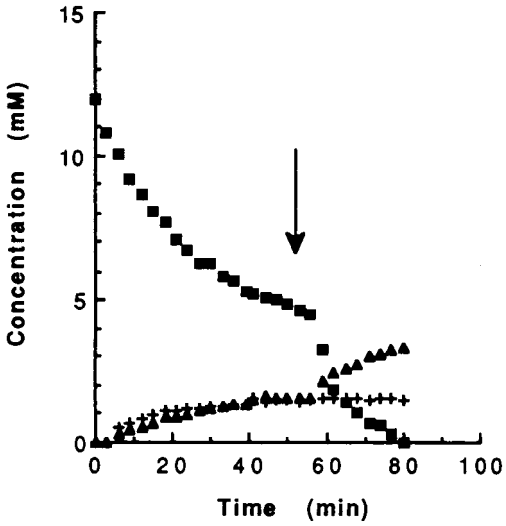

FIG. 4. Kinetics of [2-^{13}C]glucose (12 mM) consumption at pH 4.0. At the time indicated by the arrow, unlabeled citrate (5 mM) was added. The data were extracted from the in vivo ^{13}C NMR spectra as described in Materials and Methods. Symbols: ■, glucose; ▲, acetate; +, ethanol.

tate as an illustration, the central singlet at 1.9 ppm was assigned to the unlabeled isotopomer of acetic acid, CH_3COOH; the two lateral resonances were due to the labeled methyl group of acetate with no adjacent ^{13}C nuclei, $^{13}CH_3COOH$; and the inner doublet split by a small coupling constant was due to unlabeled methyl protons covalently bound to a ^{13}C nucleus, $CH_3{}^{13}COOH$. The resonance patterns due to the methyl groups of lactate and 2,3-butanediol are also highlighted in this spectrum.

The analysis of these supernatant solutions by ^{1}H- and ^{13}C-NMR allowed precise determination of the origin of each of the carbon atoms in the end products by the following strategy: the metabolism of [2,4-^{13}C]citrate is expected to produce lactate, acetate, and C_4 compounds labeled on the CH_3 groups. In addition, the presence of label on the two moieties of glucose allowed us to differentiate between the products derived from the cleavage of xylulose-5-phosphate by phosphoketolase. In fact, acetylphosphate derived from [2-^{13}C]glucose will produce acetate labeled on the CH_3 group, whereas the label from the C-5 position will end up in the COOH group of acetate and in the CHOH groups of lactate and 2,3-butanediol. The CH_3 group of acetate will also be labeled from [2,4-^{13}C]citrate. However, it is possible to determine how much label is derived from each substrate, taking into account that the ratio of isotopic enrichment on C-2 and C-1 of the pool of acetate which is derived from pyruvate must be equal to the ratio of isotopic enrichment on C-3 and C-2 of lactate, since both end products are derived from the same pyruvate pool. The determination of this ratio is straightforward from the quantification of the C_3 and C_2 resonances because of lactate in the ^{13}C-NMR spectrum of the supernatant solution (Fig. 5), after correction for the contribution of the natural abundance pool that can be determined from the ^{1}H-NMR spectrum. The value found for this ratio was 3.87 (the mean of two independent experiments). Moreover, since identical amounts of [2-^{13}C]glucose and [5-^{13}C]glucose were supplied and no ethanol was produced, the amount of acetate labeled on the CH_3 group and derived from [2-^{13}C]glucose must be equal to the total amount of label present in the COOH group of acetate plus the CHOH group of lactate and 2,3-butanediol. The amount of acetate resulting from the initial cleavage of citrate was calculated by subtracting the CH_3-labeled acetate, derived from either [2-^{13}C]glucose or [3-^{13}C]pyruvate, from the total pool of CH_3-labeled acetate, which was directly determined from proton spectra. From these relationships, it was possible to determine fluxes through the several branching points and therefore, for each of the end products, to determine the amount of products derived from the substrates supplied and from the endogenous reserves (Fig. 6).

Figure 7 shows the end products derived from citrate or glucose during citrate-glucose cometabolism, as well as the products of the metabolism of citrate in an experiment in which [2,4-^{13}C]citrate was the sole carbon source. The carbon recoveries from citrate and glucose were approximately 72 and 65%, respectively. Taking into account the unlabeled end products derived from the catabolism of supplied glucose, it was found that 18 μmol of acetate plus lactate · min^{-1} · g (dry mass) of $cells^{-1}$ was derived from the mobilization of endogenous compounds.

Pools of phosphorylated intermediates during glucose, citrate-glucose, and citrate metabolism. ^{31}P-NMR spectra of extracts obtained during the metabolism of citrate, glucose, and citrate-glucose at pH 4.0 by *L. oenos* are shown in Fig. 8. The resonances due to the phosphate groups of nucleoside triphosphates (e.g., ATP) were detected in the extract obtained from cells cometabolizing citrate plus glucose (Fig. 8C) or citrate alone (Fig. 8A), whereas in the extract obtained during the metabolism of glucose alone (Fig. 8B), those resonances were not found. The following phosphomonoesters were identified: 6-phosphogluconate, glucose-6-phosphate, glycerol-3-phosphate, 3-phosphoglycerate, AMP, 2-phosphoglycerate, and $NADP^+$. During the metabolism of glucose as the sole carbon source, the intracellular concentration of glucose-6-phosphate was 10-fold higher than the value found when citrate was also added (Table 1); as expected, the intracellular concentration of this metabolite was much lower when citrate alone was supplied. The AMP concentration was higher in the extract obtained from cells metabolizing glucose alone (1.2 mM) than in cells utilizing citrate plus glucose (0.29 mM).

ATP levels developed in cell suspensions of *L. oenos* metabolizing citrate, glucose-citrate, or glucose were measured, in independent experiments, as a function of time after the addition of substrates. The results obtained after 10 min of incubation are shown in Fig. 9. The ATP level measured in cells metabolizing glucose was very low, whereas during citrate-glucose cometabolism, the ATP concentration was increased by a factor of 11-fold. An intermediate situation was found in cells utilizing citrate alone, for which a concentration of ATP fourfold higher than the value obtained during the metabolism of glucose as the sole carbon source was measured.

DISCUSSION

NMR coupled with the utilization of ^{13}C-enriched substrates allowed identification and discrimination between the products derived from the metabolism of citrate and glucose and also from those derived from endogenous reserve compounds. This information is accessible by other analytical techniques only if the carbon recoveries are complete (100%) for all substrates and the contribution of the metabolism of internal reserves is negligible. Relatively low recoveries were in fact obtained in the experiments in which isotopically enriched substrates were used, most probably because of deviation of metabolic intermediates to biosynthesis. The carbon recoveries in the experiments with nonlabeled substrates appear to be significantly higher, but these values are misleading, since the contribution

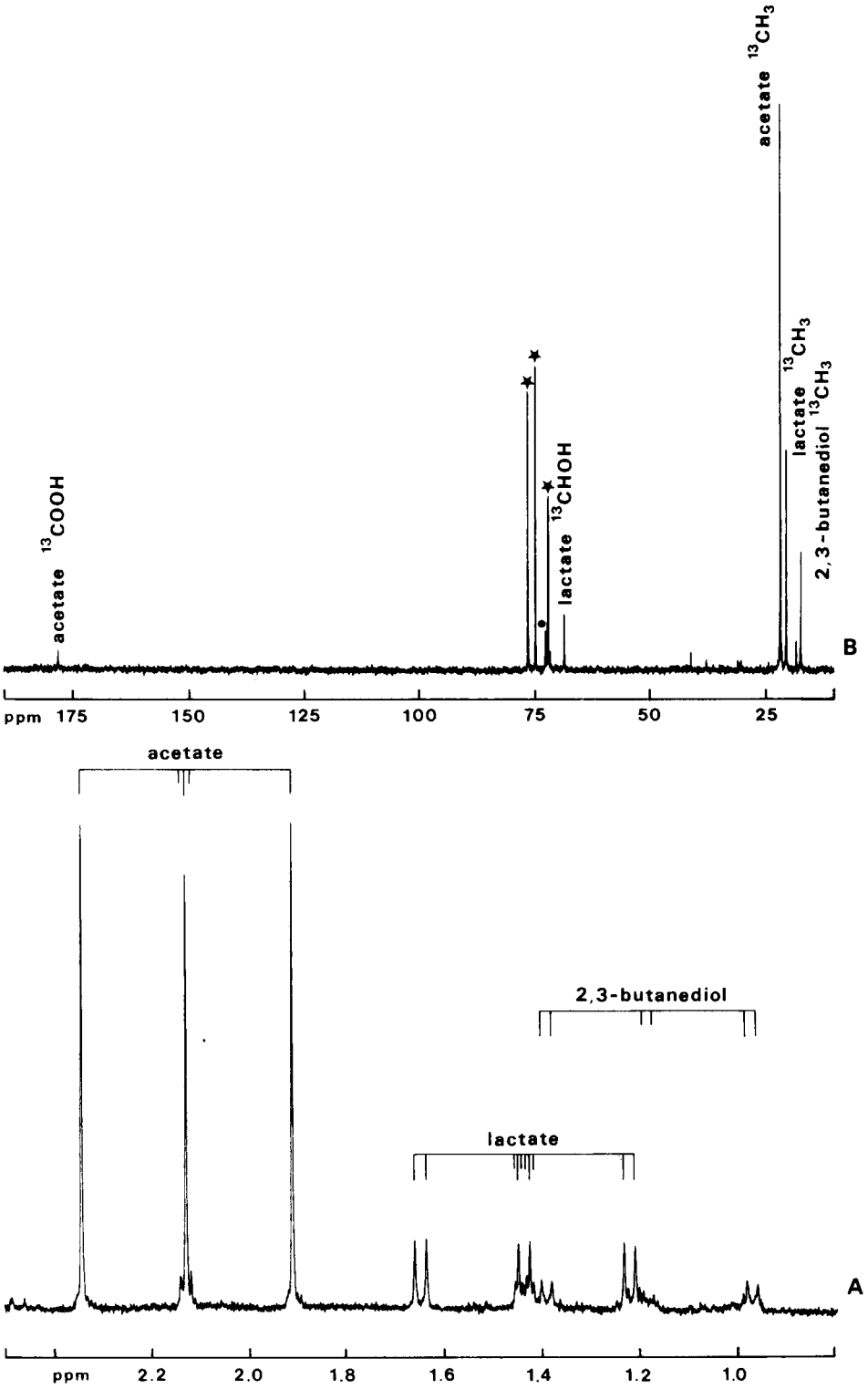

FIG. 5. ^{1}H (A) and fully relaxed proton-decoupled ^{13}C (B) NMR spectra of a cell supernatant containing the fermentation products from the cometabolism of [2-^{13}C]glucose–[5-^{13}C]glucose (10.2 μmol) and [2,4-^{13}C]citrate (15.9 μmol). Symbols in the ^{13}C spectrum: *, glucose; ●, $^{13}CHOH$ groups of 2,3-butanediol. The resonance patterns due to methyl groups of acetate, lactate, and 2,3-butanediol are indicated in the proton spectrum.

from the products derived from the internal reserves could not be subtracted. Therefore, the use of labeling experiments coupled to NMR is essential for a correct description of metabolism. In our previous studies with *Lactococcus lactis* (15), a comparison was made between the metabolic behavior of growing and nongrowing cells by this NMR approach. The main conclusion was that carbon was metabolized in similar ways in the two cases; therefore, it is expected that the results

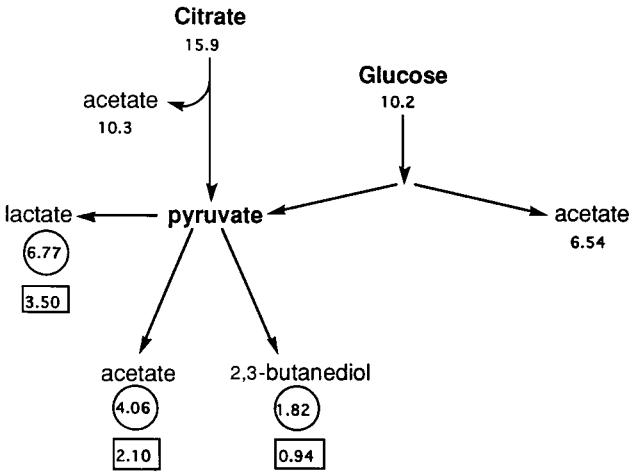

FIG. 6. Carbon fluxes through the branching points of citrate-glucose cometabolism. The amounts (in micromoles) of each end product derived from citrate (circles) and glucose (squares) are discriminated.

presented here for *L. oenos* will provide a significant picture of carbon routing under growing conditions.

The data concerning mobilization of reserve compounds are in agreement with our previous results (15, 16). Attempts to extract and identify the reserve compound(s) in *L. oenos* have not been successful so far; however, biosynthesis of intracellular glycogenlike α-1,4-glucans has been reported for some strains of oral streptococci (1, 7).

A strong interrelationship between the metabolism of citrate and hexoses was observed, resulting in considerable differences in the nature and molar ratios of end products. Carbon from citrate was channelled to lactate and 2,3-butanediol when glucose was present, whereas acetoin was the main product of the metabolism of citrate alone (Fig. 7). On the other hand, the presence of citrate induced a shift from the heterofermentative metabolism of glucose: acetate accounted for approximately 65% of the end products (molar basis) derived from glucose, whereas in the absence of citrate, the contribution of acetate was at most 38% and ethanol, erythritol, and glycerol represented ca. 60% of the products (24). Taken together, the results show that the metabolism of citrate confers additional pathways for reoxidation of NAD(P)H; the metabolic flux from pyruvate is directed toward the production of 2,3-butanediol (via α-acetolactate synthase, α-acetolactate decarboxylase, and acetoin reductase) and toward lactate (via lactate dehydrogenase). This allows diversion of sugar carbon to reactions in which ATP is synthesized, with consequent formation of acetate instead of ethanol.

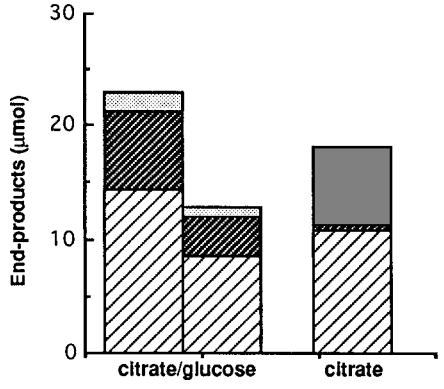

FIG. 7. Pattern of end products formed at 30°C and pH 4.0 by a cell suspension of *L. oenos* from [2,4-^{13}C]citrate (15.9 μmol) and [2-^{13}C]glucose–[5-^{13}C]glucose (10.2 μmol) cometabolism and [2,4-^{13}C]citrate (16 μmol) as the sole carbon source. Symbols: ▨, acetate; ▨, lactate; ▨, 2,3-butanediol; ▨, acetoin.

When citrate-glucose or citrate-fructose cometabolism was monitored in dilute cell suspensions of *L. oenos*, the pattern of end product formation was similar to that found in the analogous experiments with in vivo NMR. The transient accumulation of acetoin during citrate-fructose cometabolism is explained by the reduction of part of the fructose to mannitol, concomitant with NAD(P)$^+$ formation (24), which results in a lesser need to regenerate NAD(P)$^+$. The results obtained when citrate-arabinose cometabolism was probed in dilute cell suspensions support this hypothesis: arabinose entered the heterofermentative pathway at the level of xylulose-5-phosphate, and no reduced cofactors were formed (Fig. 3); as a result, no 2,3-butanediol was produced.

Recently, Salou et al. (20) have reported on citrate-sugar metabolism by growing cells of *L. oenos*. In their study, an equimolar conversion of citrate to acetate, lactate, and carbon dioxide was assumed, and the production of 2,3-butanediol was not assessed, making a comparison with our results difficult.

In *Leuconostoc mesenteroides* and *Leuconostoc lactis*, citrate is also converted mainly to acetate and lactate during citrate-glucose cometabolism, but only minor amounts of C_4 compounds (acetoin, diacetyl, or 2,3-butanediol) are produced (2, 22), in contrast with the observations for *L. oenos*. The metabolic differences found between *L. oenos* and leuconostocs isolated from dairy sources are not surprising, since this bacterium belongs to a widely separated cluster (8), which led to the recently proposed reclassification of *L. oenos* as *Oenococcus oeni* (5).

The intracellular accumulation of glucose-6-phosphate during the metabolism of glucose is consistent with a high intracellular NAD(P)H/NAD(P)$^+$ ratio, which inhibits glucose-6-phosphate dehydrogenase and 6-phosphogluconate dehydrogenase (26). However, when citrate was cometabolized with glucose, the ratio decreased, as did the intracellular concentration of glucose-6-phosphate (Table 1), a result interpreted here as being caused by relief of the inhibition in the above-mentioned enzymes; this is also in accordance with the citrate-induced stimulation of the glucose consumption rate observed in the experiment in Fig. 4.

It has been postulated that in heterofermentative lactic acid bacteria, the citrate-induced growth enhancement is due to the increased ATP yield from glucose formed by substrate-level phosphorylation in the reaction catalyzed by acetate kinase (2, 20, 23). In fact, the increased intensities of the resonances due to nucleoside triphosphates observed in the spectrum of the extract obtained during citrate-glucose cometabolism (Fig. 8C) when compared with the extract obtained from cells metabo-

TABLE 1. Intracellular concentration of phosphomonoesters produced during *L. oenos* metabolism of glucose, glucose plus citrate, and citrate alone

Substrate	Concn (mM) of phosphomonoester[a]:					
	6-PG	G-6-P	G-3-P	3-PGA	AMP	NADP+/2-PGA
Glucose	0.5	1.1	0.5	0.6	1.2	0.3
Glucose-citrate	0.4	0.1	0.3	2.4	0.3	0.4
Citrate	0.2	0.2	0.4	1.4	0.8	0.4

[a] Abbreviations are as in the legend to Fig. 8.

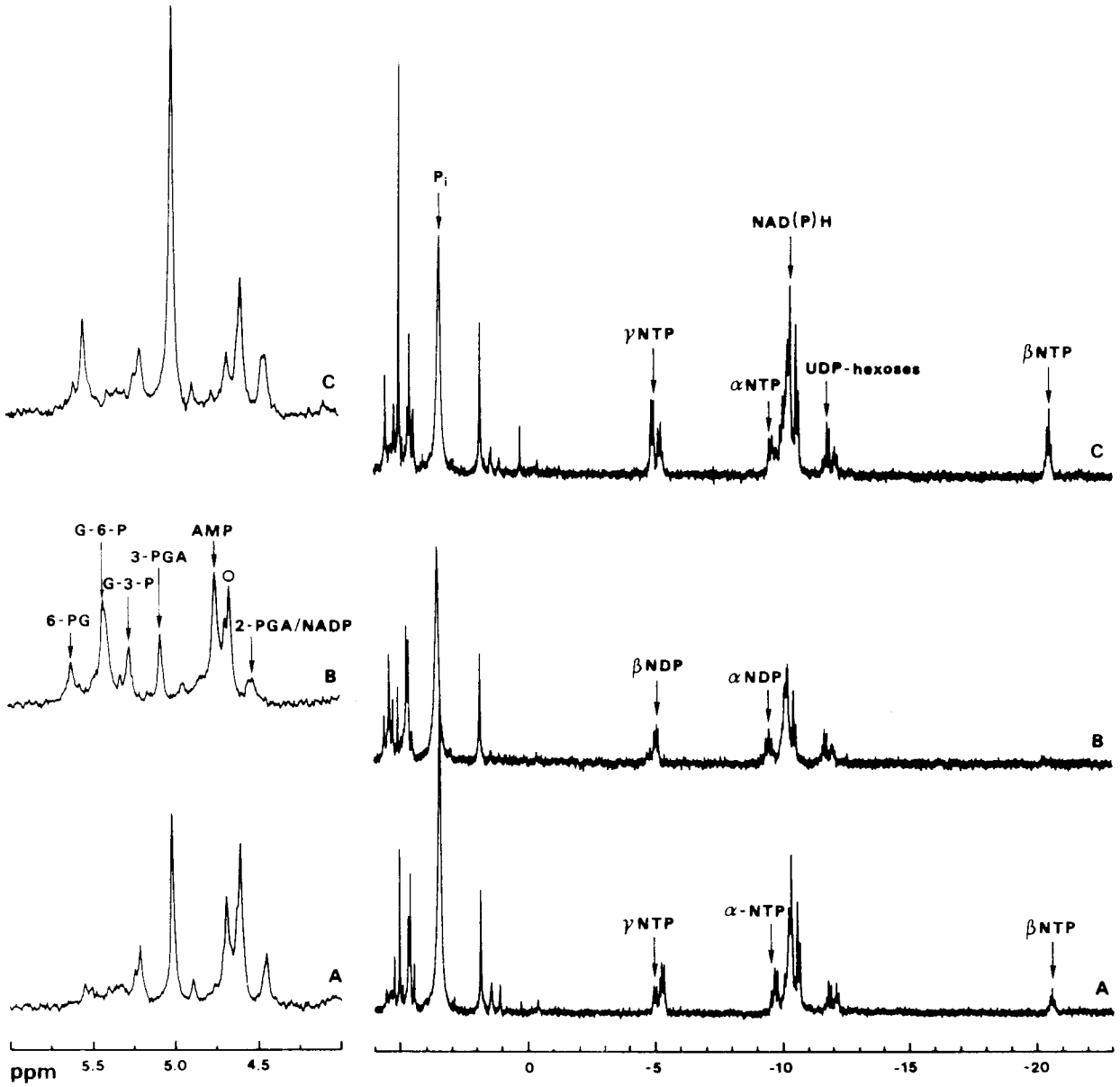

FIG. 8. ^{31}P NMR spectra of perchloric acid extracts of cell suspensions of *L. oenos* metabolizing citrate (A), glucose (B), and citrate plus glucose (C). A horizontal expansion of the phosphomonoester region (6 to 4 ppm) is also shown. Chemical shifts (in ppm) of the identified resonances: 6-phosphogluconate (6-PG) at 5.6, glucose-6-phosphate (G-6-P) at 5.4 and 5.3, glycerol-3-phosphate (G-3-P) at 5.2, 3-phosphoglycerate (3-PGA) at 5.0, AMP at 4.7, and 2-phosphoglycerate (2-PGA)/$NADP^+$ at 4.5. ○, unassigned resonances; αNTP, βNTP, and γNTP, resonances of nucleoside triphosphates; αNDP and βNDP, resonances of nucleoside diphosphates.

lizing glucose alone (Fig. 8B) is consistent with that explanation. The increased ATP yield from glucose during citrate-glucose cometabolism was fully confirmed by the results shown in Fig. 9. Furthermore, high levels of ATP derived from the metabolism of citrate alone were observed (compare bars C and A in Fig. 9). In *L. oenos*, uniport of the monoanionic species of citrate and further metabolism generate a proton motive force composed of both a transmembrane electrical potential and a pH gradient (17); the production of ATP from citrate metabolism at low pH, when acetate formation via acetate kinase is negligible (16), shows that the generated proton motive force is high enough to drive ATP synthesis. In agreement with this proposal is the observed growth on FT80 medium with citrate as the sole added carbon source, although attempts to grow *L. oenos* on defined medium containing citrate but no carbohydrates were not successful. This may be due to the inability of these organisms to perform gluconeogenesis and therefore to grow in the absence of sugars. The energy generated by the secondary transport of citrate will supplement the energy obtained from glucose by substrate-level phosphorylation, and this has important consequences for the survival and competitiveness of *L. oenos* in wine.

In summary, this work has uncovered the important role of citrate in the bioenergetics of *L. oenos*, as well as in affecting the nature and proportions of end products derived from three major sugars present in wine after the ethanol fermentation. These metabolic features and the energetic gain are now understood. Furthermore, the use of ^{13}C labeling to measure

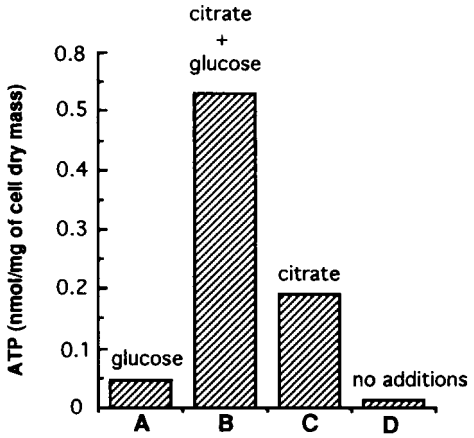

FIG. 9. ATP levels in *L. oenos* after incubation at pH 4.0 with 10 mM glucose (A), 5 mM citrate plus 10 mM glucose (B), 5 mM citrate (C), or no additions (D).

carbon fluxes in this organism is demonstrated. This type of knowledge is an essential step toward a full control of malolactic fermentation and of the final organoleptic properties of wine, and it provides useful metabolic directives for improvement of starter cultures.

ACKNOWLEDGMENTS

This work was supported by the Biotechnology (BRIDGE) Program, contract BIOT-CT91-0263, of the Commission of the European Communities and by Junta Nacional de Investigação Científica e Tecnológica (JNICT), Portugal, grant STRDA/C/BIO/355/92. A. Ramos is grateful to JNICT for the award of a doctoral fellowship.

We thank Dulce Brito for the use of the bioluminometer and Vitória SanRomão and Cristina Leitão for their support in high-performance liquid chromatography determinations.

REFERENCES

1. **Birkhed, D., and J. M. Tanzer.** 1979. Glycogen synthesis pathway in *Streptococcus mutans* strain NCTC 10449S and its glycogen synthesis defective mutant 805. Arch. Oral Biol. **24:**67–73.
2. **Cogan, T. M.** 1987. Co-metabolism of citrate and glucose by *Leuconostoc* spp.: effects on growth, substrates, and products. J. Appl. Bacteriol. **63:**551–558.
3. **Cogan, T. M., M. O'Dowd, and D. Mellerick.** 1981. Effects of pH and sugar on acetoin production from citrate by *Leuconostoc lactis*. Appl. Environ. Microbiol. **41:**1–8.
4. **Davis, C. R., D. Wiwobo, R. Eschenbruch, G. H. Fleet, and T. H. Lee.** 1985. Practical implications of malolactic fermentation: a review. Am. J. Enol. Vitic. **36:**290–301.
5. **Dicks, L. M. T., F. Dellaglio, and M. D. Collins.** 1995. Proposal to reclassify *Leuconostoc oenos* as *Oenococcus oeni* [corrig.] gen. nov., comb. nov. Int. J. Syst. Bacteriol. **45:**395–397.
6. **Fornachon, J. C. M., and B. Lloyd.** 1965. Bacterial production of diacetyl and acetoin in wine. J. Sci. Food Agric. **19:**374–378.
7. **Hamilton, I. R.** 1968. Synthesis and degradation of intracellular polyglucose in *Streptococcus salivarius*. Can. J. Microbiol. **14:**65–77.
8. **Holzapfel, W. H., and U. Schillinger.** 1992. The genus *Leuconostoc*, p. 1508–1534. *In* A. Balows, H. G. Trüper, M. Dworkin, W. Harder, and K. H. Schleifer, The Prokaryotes, vol. II, 2nd ed. Springer-Verlag, New York.
9. **Kanodia, S., and M. Roberts.** 1983. Methanophosphagen: unique cyclic pyrophosphate isolated from *Methanobacterium thermoautotrophicum*. Proc. Natl. Acad. Sci. USA **80:**5217–5221.
10. **Lindgren, S. E., L. T. Axelsson, and R. F. McFeeters.** 1990. Anaerobic L-lactate degradation by *Lactobacillus plantarum*. FEMS Microbiol. Lett. **66:**209–214.
11. **Lonvaud-Funel, A.** 1986. Ph.D. thesis. Université de Bordeaux II, Bordeaux, France.
12. **Lonvaud-Funel, A., C. Zmirou, and F. Weinzorm.** 1984. Le métabolisme de lácide citrique par les bactéries lactiques de la fermentation malolactique des vins. Sci. Aliments **4:**81–85.
13. **McFeeters, R. F., and K. Chen.** 1986. Utilization of electron acceptors for anaerobic mannitol metabolism by *Lactobacillus plantarum*. Compounds which serve as electron acceptors. Food Microbiol. **3:**73–81.
14. **Otto, R., B. Klont, B. ten Brink, and W. N. Konings.** 1984. The phosphate potential, adenylate energy charge and proton motive force in growing cells of *Streptococcus cremoris*. Arch. Microbiol. **139:**338–343.
15. **Ramos, A., K. N. Jordan, T. M. Cogan, and H. Santos.** 1994. ^{13}C nuclear magnetic resonance studies of citrate and glucose cometabolism by *Lactococcus lactis*. Appl. Environ. Microbiol. **60:**1739–1748.
16. **Ramos, A., J. S. Lolkema, W. N. Konings, and H. Santos.** 1995. An enzyme basis for pH regulation of citrate and pyruvate metabolism by *Leuconostoc oenos*. Appl. Environ. Microbiol. **61:**1303–1310.
17. **Ramos, A., B. Poolman, H. Santos, J. S. Lolkema, and W. N. Konings.** 1994. Uniport of anionic citrate and proton consumption in citrate metabolism generate a proton motive force in *Leuconostoc oenos*. J. Bacteriol. **176:**4899–4905.
18. **Ribéreau-Gayon, J., E. Peynaud, P. Ribéreau-Gayon, and P. Sudraud.** 1975. Sciences et techniques du vin, vol. 2. Dunod, Paris.
19. **Rogosa, M., J. G. Franklin, and K. D. Perry.** 1961. Correlation of the vitamin requirements with cultural and biochemical characters of *Lactobacillus* spp. J. Gen. Microbiol. **25:**473–482.
20. **Salou, P., P. Loubiere, and A. Pareilleux.** 1994. Growth and energetics of *Leuconostoc oenos* during cometabolism of glucose with citrate or fructose. Appl. Environ. Microbiol. **60:**1459–1466.
21. **Schmitt, P., and C. Diviès.** 1991. Co-metabolism of citrate and lactose by *Leuconostoc mesenteroides* subsp. *cremoris*. J. Ferment. Bioeng. **71:**72–74.
22. **Schmitt P., C. Diviès, and R. Cardona.** 1992. Origin of end-products from the co-metabolism of glucose and citrate by *Leuconostoc mesenteroides* subsp. *cremoris*. Appl. Microbiol. Biotechnol. **36:**679–683.
23. **Starrenburg, M. J. C., and J. Hugenholtz.** 1991. Citrate fermentation by *Lactococcus* and *Leuconostoc* spp. Appl. Environ. Microbiol. **57:**3535–3540.
24. **Veiga-da-Cunha, M., P. Firme, M. V. SanRomão, and H. Santos.** 1992. Application of ^{13}C nuclear magnetic resonance to elucidate the unexpected biosynthesis of erythritol by *Leuconostoc oenos*. Appl. Environ. Microbiol. **58:**2271–2279.
25. **Veiga-da-Cunha, M., and M. A. Foster.** 1992. Sugar-glycerol cofermentations in lactobacilli: the fate of lactate. J. Bacteriol. **174:**1013–1019.
26. **Veiga-da-Cunha, M., H. Santos, and E. van Schaftingen.** 1993. Pathway and regulation of erythritol formation in *Leuconostoc oenos*. J. Bacteriol. **175:**3941–3948.
27. **Wiwobo, D., R. Eschenbruch, C. R. Davis, H. Fleet, and T. H. Lee.** 1985. Occurrence and growth of lactic acid bacteria in wine: a review. Am. J. Enol. Vitic. **36:**302–313.